

Dynamical effects of the spiral arms on the velocity distribution of disc stars

Kohei Hattori¹, Naoteru Gouda², Taihei Yano², Nobuyuki Sakai² and Hiromichi Tagawa²

¹University of Michigan, 1085 S. University Ave, Ann Arbor, MI 48109, USA
email: khattori@umich.edu

²National Astronomical Observatory of Japan, 2-21-1, Osawa, Mitaka, Tokyo 181-8588, Japan

Abstract. Nearby disc stars in Gaia DR1 (TGAS) and RAVE DR5 show a bimodal velocity distribution in the metal-rich region (characterized by the Hercules stream) and mono-modal velocity distribution in the metal-poor region. We investigate the origin of this [Fe/H] dependence of the local velocity distribution by using 2D test particle simulations. We found that this [Fe/H] dependence can be well reproduced if we assume fast rotating bar models with $\Omega_{\text{bar}} \simeq 52 \text{ km s}^{-1} \text{ kpc}^{-1}$. A possible explanation for this result is that the metal-rich, relatively young stars are more likely to be affected by bar's outer Lindblad resonance due to their relatively cold kinematics. We also found that slowly rotating bar models with $\Omega_{\text{bar}} \simeq 39 \text{ km s}^{-1} \text{ kpc}^{-1}$ can not reproduce the observed data. Interestingly, when we additionally consider spiral arms, some models can reproduce the observed velocity distribution even when the bar is slowly rotating.

Keywords. Galaxy: disk, Galaxy: kinematics and dynamics, Galaxy: structure

1. Introduction: Does Hercules stream arise from slow-bar + spirals?

Since the discovery of the bimodal velocity distribution of the local disc stars, many authors have tried to explain the origin of the secondary peak, or the Hercules stream. The pioneering work by Dehnen (2000) demonstrated that the under-dense region between the Local Standard of Rest mode (LSR mode; first peak) and the Hercules stream (secondary peak) can arise from the bar's outer Lindblad resonance (OLR). Based on this idea, Dehnen (1999) estimated the bar's pattern speed to be $\Omega_b = (53 \pm 3) \text{ km s}^{-1} \text{ kpc}^{-1}$. Later studies refined this estimation by using other samples of nearby stars and obtained similar values of Ω_b (Minchev *et al.* 2007; Antoja *et al.* 2014; Monari *et al.* 2017).

Unfortunately, this *fast bar* model is inconsistent with recent claims of long Galactic bar (half-length of 5 kpc; Wegg *et al.* 2015). Portail *et al.* (2017) argued that slowly rotating bar with $\Omega_b = (39 \pm 3.5) \text{ km s}^{-1} \text{ kpc}^{-1}$ is required to sustain the long bar.

This $\sim 30\%$ difference in Ω_b between the *fast bar* and *slow bar* models is more serious than it sounds. For example, if $\Omega_b \simeq 39 \text{ km s}^{-1} \text{ kpc}^{-1}$ (slow bar), OLR is unimportant in the Solar neighborhood, so the bimodal structure cannot be reproduced. Here we consider bar + spiral models to investigate the origin of the Hercules stream.

2. Data: TGAS+RAVE

Here we explain the observed data with which our models are compared.

First, we cross match the sample stars in Tycho Gaia Astrometric Solutions (TGAS) from the Gaia DR1 (Lindegren *et al.* 2016) and RAVE DR5 (Kunder *et al.* 2017). Then we use the 5D astrometric data from TGAS and the line-of-sight velocity and [Fe/H] from RAVE to derive the velocity distribution of stars within 200 pc from the Sun. Our sample is defined by the following criteria: (1) positive parallax ($\varpi > 0$); (2) distance cut

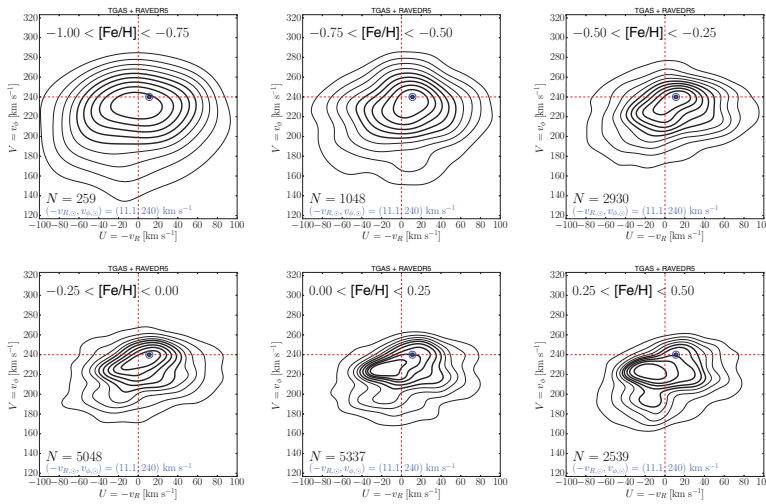


Figure 1. Distribution of nearby stars in the (U, V) -space at various $[\text{Fe}/\text{H}]$ regions revealed by Gaia (TGAS) and RAVE data. Here we assume Solar motion of $(U_{\odot}, V_{\odot}) = (11.1, 240) \text{ km s}^{-1}$.

($1/\varpi < 200 \text{ pc}$); (3) small fractional error in parallax ($\delta\varpi/\varpi < 0.2$); (4) small line-of-sight velocity error ($0 < \delta v_{\text{los}}/(\text{km s}^{-1}) < 5$); (5) metallicity cut ($-1 \leq [\text{Fe}/\text{H}] \leq 0.5$); and (6) large S/N ratio in RAVE spectra ($\text{SNR} > 40$).

Figure 1 shows the $[\text{Fe}/\text{H}]$ dependence of the velocity distribution. In the most metal-poor regions ($-1 \leq [\text{Fe}/\text{H}] \leq -0.75$ and $-0.75 \leq [\text{Fe}/\text{H}] \leq -0.5$), we see a mono-modal distribution, which is associated with a large velocity dispersion (hot kinematics). As the $[\text{Fe}/\text{H}]$ increases, the velocity dispersion becomes smaller (colder kinematics). At the most metal-rich regions ($0 \leq [\text{Fe}/\text{H}] \leq 0.25$ and $0.25 \leq [\text{Fe}/\text{H}] \leq 0.5$), we see a clear secondary peak at $(U, V) = (-10, 195) \text{ km s}^{-1}$ (see also Pérez-Villegas *et al.* 2017).

3. Model

Here we describe our 2D test particle simulations. We assume that the stellar disc is formed at $t = -12 \text{ Gyr}$ and that the star formation rate is constant as a function of time, t . Initially, the stellar disc is axisymmetric, and the non-axisymmetric components are adiabatically introduced at $t = T_{\text{form}}$. At $t < T_{\text{form}}$, we assume that the stellar disc is evolved due to internal heating. At $T_{\text{form}} < t$, we follow the stellar orbits. Also, we use a simple model to assign the metallicity of stars based on the initial radius and the age.

The Galactic potential is modeled by the following components:

Axisymmetric component. For this component, we assume a singular isothermal potential of $\Phi_0(R) = v_0^2 \ln(R/R_0)$ with $(R_0, v_0) = (8 \text{ kpc}, 220 \text{ km s}^{-1})$.

Bar component. We assume a quadratic bar model introduced by Dehnen (2000), with the bar strength of $\alpha = 0.015$ (for bar-only models) or $\alpha = 0.01$ (for bar+spiral models). The current bar’s angle with respect to the Sun-Galactic center line is set to be 25° .

Spiral component. We assume rigidly-rotating, two- or four-armed ($m = 2, 4$) logarithmic spirals. The maximum amplitude of the spiral potential at $R = R_0$ is $(20 \text{ km s}^{-1})^2$ and $(15 \text{ km s}^{-1})^2$ for $m = 2$ and 4, respectively. The amplitude is varied as a function of R , in a manner that is motivated by Steiman-Cameron *et al.* (2010). We consider steady spirals without t -dependence of the amplitude, as well as transient spirals where the amplitude oscillates with a period of 200 Myr. In all the models, one of the spirals at $R = R_0$ is currently located at 45° ahead of the Sun.

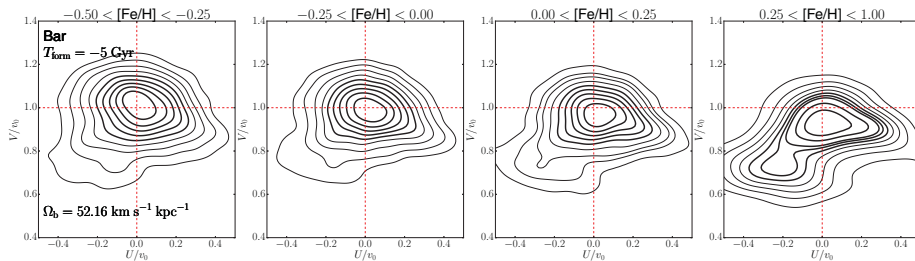


Figure 2. $[\text{Fe}/\text{H}]$ dependence of the (U, V) -diagram in the fast-bar model ($T_{\text{form}} = -5$ Gyr).

4. Results

Fast-bar model (no spirals). In the fast-bar model ($\Omega_b = 52.16 \text{ km s}^{-1} \text{ kpc}^{-1}$), a prominent bimodal structure is seen at the metal-rich region but is not seen in metal-poor region (Fig 2), almost independent of T_{form} . The value of V that separates the LSR and Hercules-like modes corresponds to the bar's OLR. These results are consistent with the Gaia+RAVE data (Fig 1). A possible explanation for these results is as follows: Disc stars with high (low) $[\text{Fe}/\text{H}]$ tend to be young (old) and have cold (hot) kinematics, so they are more (less) likely to be affected by OLR. However, further investigation is required for a better understanding of these results.

Slow-bar model (no spirals). In the slow-bar model ($\Omega_b = 39.12 \text{ km s}^{-1} \text{ kpc}^{-1}$), in contrast, we do not see bimodal structure in any $[\text{Fe}/\text{H}]$ range.

Slow-bar + steady spirals. When $m = 4$ and $\Omega_s = 20 \text{ km s}^{-1} \text{ kpc}^{-1}$, the $[\text{Fe}/\text{H}]$ dependence of the (U, V) -diagram is similar to the observed one for certain values of T_{form} (Fig 3, top row); but if we slightly change T_{form} , we see bimodal structure not only in metal-rich region but also in metal-poor region (Fig 3, bottom row), unlike Gaia data. It turned out that when bar and spirals have different pattern speeds, most of the disc orbits become chaotic. It seems that the $[\text{Fe}/\text{H}]$ dependence of the bimodality behaves in a unpredictable manner due to the chaotic nature of disc orbits. Interestingly, the value of V that separates the two modes is the spiral's 4:1 inner Lindblad resonance (ILR), almost independent of T_{form} . Therefore, the observed location of the Hercules stream may indicate the spiral's nature (Ω_s that determines ILR in this model), while the $[\text{Fe}/\text{H}]$ dependence of the bimodality is uninformative. Therefore, in this case we should not over-interpret the $[\text{Fe}/\text{H}]$ dependence of the Hercules stream.

Slow-bar + transient spirals. When $m = 2$ and $\Omega_s = 25 \text{ km s}^{-1} \text{ kpc}^{-1}$, the $[\text{Fe}/\text{H}]$ dependence of the (U, V) -diagram is similar to the observed one for certain values of T_{form} (Fig 4); but it is not the case for other values of T_{form} . Again, it seems this unpredictable $[\text{Fe}/\text{H}]$ dependence of the bimodal structure is due to the chaoticity of disc orbits. Interestingly, the value of V of the secondary peak approximately satisfy a condition of (stellar radial period) \simeq (spiral's half-period) ($= 100$ Myr in our case), almost independent of T_{form} . Therefore, the observed location of the Hercules stream may indicate the spiral's properties (lifetime of the spirals in this model).

5. Conclusions

We show that fast-bar model can reproduce the observed $[\text{Fe}/\text{H}]$ dependence of the local velocity distribution, while slow-bar model fails to explain it.

Also, when spiral arms are additionally considered, some models can explain the observed data even when the bar is slowly rotating. In such cases, the location of the bimodal structure may indicate some properties of spiral arms, such as Ω_s or the lifetime

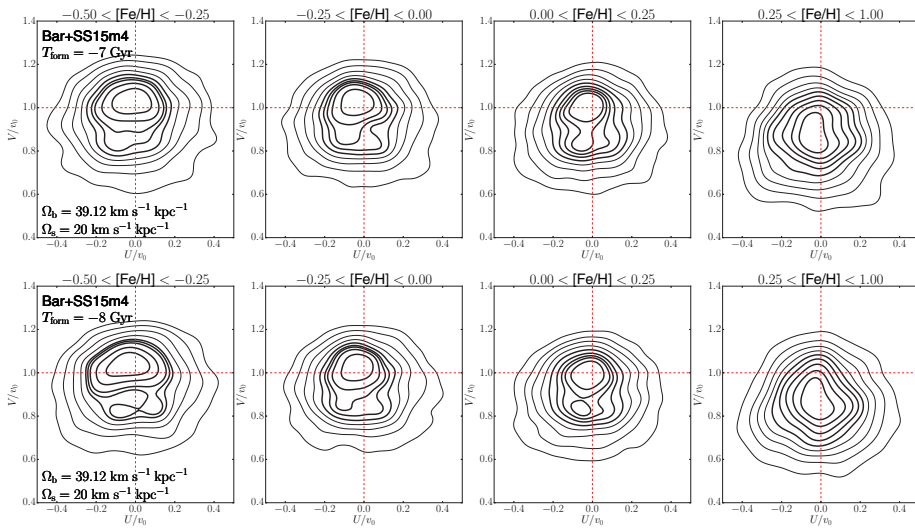


Figure 3. Slow-bar+steady spiral model ($m = 4$). ($T_{\text{form}} = -7$ Gyr (top), -8 Gyr (bottom)).

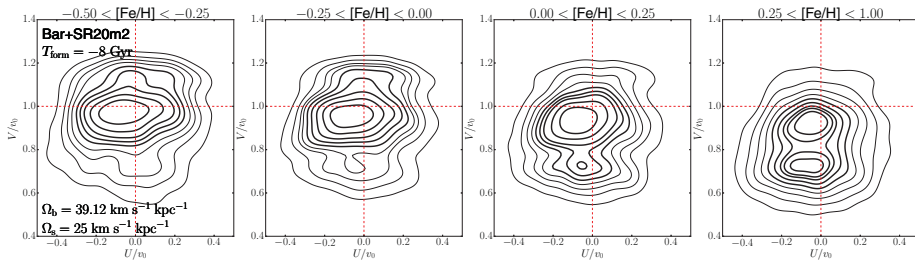


Figure 4. Slow-bar+transient spiral model ($m = 2$, $T_{\text{form}} = -8$ Gyr).

of the spiral arms. However, in such cases, due to the chaotic nature of disc orbits, we should not over-interpret the $[\text{Fe}/\text{H}]$ dependence of the bimodality.

Acknowledgments. This work has made use of data from the European Space Agency (ESA) mission *Gaia* (<https://www.cosmos.esa.int/gaia>), processed by the *Gaia* Data Processing and Analysis Consortium (DPAC, <https://www.cosmos.esa.int/web/gaia/dpac/consortium>). Funding for the DPAC has been provided by national institutions, in particular the institutions participating in the *Gaia* Multilateral Agreement. KH was supported by a grant from the Hayakawa Satio Fund awarded by the Astronomical Society of Japan.

References

- Antoja, T., Helmi, A., Dehnen, W., *et al.* 2014, *A&A*, 563, A60
 Dehnen, W. 1999, *ApJ*, 524, L35
 Dehnen, W. 2000, *AJ*, 119, 800
 Kunder, A., Kordopatis, G., Steinmetz, M., *et al.* 2017, *AJ*, 153, 75
 Lindegren, L., Lammers, U., Bastian, U., *et al.* 2016, *A&A*, 595, A4
 Minchev, I., Nordhaus, J., & Quillen, A. C. 2007, *ApJ*, 664, L31
 Monari, G., Kawata, D., Hunt, J. A. S., & Famaey, B. 2017, *MNRAS*, 466, L113
 Pérez-Villegas, A., Portail, M., Wegg, C., & Gerhard, O. 2017, *ApJ*, 840, L2
 Portail, M., Gerhard, O., Wegg, C., & Ness, M. 2017, *MNRAS*, 465, 1621
 Steiman-Cameron, T. Y., Wolfire, M., & Hollenbach, D. 2010, *ApJ*, 722, 1460
 Wegg, C., Gerhard, O., & Portail, M. 2015, *MNRAS*, 450, 4050